Microchimica Acta (2023) 190:270
https://doi.org/10.1007/s00604-023-05846-4

ORIGINAL PAPER

N,N-dicarboxymethyl Perylene-diimide-modified CdV2O6 Nanorods for Colorimetric Sensing of H_2O_2 and Pyrogallol

Yaru Liu[1] · Pingping Hao[1] · Liming Wang[1] · Guijiang Li[1,2] · Gaochao Fan[2] · Tao Wu[1] · Xixi Zhu[1] · Qingyun Liu[1]

Received: 20 January 2023 / Accepted: 20 May 2023 / Published online: 21 June 2023

Abstract

The peroxidase-like activity of CdV_2O_6 nanorods has been considerably improved by modification with N, N-dicarboxymethyl perylene-diimide (PDI) as a photosensitizer. The peroxidase-like behaviors are evaluated by virtue of the colorless chromogenic substrate 3,3',5,5'-tetramethylbenzidine (TMB), which is fast changed into blue oxTMB in the presence of H_2O_2 in only 90 s. PDI-CdV_2O_6 exhibits high stability at elevated temperatures and PDI-CdV_2O_6 retains more than 70% of its catalytic activity over a wide range of 15 to 60 °C. The catalytic mechanism of PDI-CdV_2O_6 is ascribed to the synergistic interaction between PDI and CdV_2O_6 and the generation of $\bullet O_2^-$ radicals. Based on the enhanced peroxidase-like activity of PDI-CdV_2O_6, a selective colorimetric sensor has been constructed for H_2O_2 and pyrogallol (PG) with detection limits of 36.5 μM and 0.179 μM, respectively. The feasibility of the proposed sensing platform has been validated by detecting H_2O_2 in milk and pyrogallol in tap water.

Keywords PDI-CdV_2O_6 · Nanozyme · Peroxidase · Catalytic activity · Colorimetry · Photometry

Introduction

Natural enzymes have been widely studied and applied owing to their high catalytic efficiency and substrate specificity [1]. However, they usually face with some disadvantages of high extraction and purification cost, low yield and strict storage conditions, restricting their practical application [2]. As we know, artificial nanozymes can overcome such shortcoming of natural enzymes. Thereof, nanozymes have aroused considerable interests [3]. Over the past decades, scientists have prepared numerous nanomaterials including metal oxides [4], metal sulfides [5], noble metals [6], carbon-based materials [7] and metal–organic frameworks [8]. However, how to improve the catalytic activity of nanozymes is an urgent task. Scientists have put forward different strategies for improving the catalytic activity of nanozymes. For example, various composites with the high activity have been prepared, such as Co-CeO_2 [9], AgNPs@rGO [10], and Fe_3O_4@MoS_2-Ag [11], etc. What's more, to solve the agglomeration of inorganic nanoparticles, some supports were employed to disperse nanoparticles to expose more active sites and then improve the corresponding catalytic activity [12, 13]. Interestingly, some organic conjugate macromolecules as photosensitizers were used to modify the nanomaterials with semiconductivity [14, 15]. The synergistic effect between photosensitizers and nano-semiconductors would enhance the corresponding catalytic activity. Especially, Perylene diimide (PDI), as one of typical photosensitive molecules, was used to modify some inorganic nanomaterials to widen the absorption in visible region and widely used in organic photovoltaic [16] and electronic fields [17].

Pyrogallol (1,2,3-trihydroxybenzene, PG), a derivative of phenolic compounds, is widely used in pharmaceutical, cosmetic, plastic and other industries [18]. Also, PG is commonly used as an antioxidant and scavenger of

✉ Tao Wu
skd996233@sdust.edu.cn

✉ Xixi Zhu
zhuxixi@sdust.edu.cn

✉ Qingyun Liu
qyliu@sdust.edu.cn

[1] College of Chemical and Biological Engineering, Shandong University of Science and Technology, Qingdao 266590, People's Republic of China

[2] Shandong Key Laboratory of Biochemical Analysis, College of Chemistry and Molecular Engineering, Qingdao University of Science and Technology, Qingdao 266042, People's Republic of China

reactive oxygen species, due to intrinsic reductive properties. Because of the wide application of PG in industry, it will inevitably cause pollution to the aqueous environment [19]. Therefore, it is necessary to develop a fast cheap convenient method for determination of PG. Until now, many methods including chromatographic [20], electrochemical [21], and chemiluminescence have been developed to detect PG [22]. Although the other methods (such as chromatography or electrochemistry) are simple and inexpensive and can be routinely performed by technicians, it is not met requirements for spot testing. Thus, the colorimetric method based on the artificial peroxidase mimics (one of nanozymes) is a good substitute. However, the nanozyme-based colorimetric method for determining PG requests for some highly active nanozymes. Based on the above strategies of the catalytic activity of artificial nanozymes, an organic molecule with the larger conjugate structure, N, N-dicarboxymethyl perylene-diimide (PDI), can be used as a functional molecule to modify inorganic nanomaterials to obtain a nanozyme with the enhanced catalytic activity. Considering the rich chemical valences of V, CdV_2O_6 nanorods are expected to possess the peroxidase-like activity. Thus, if PDI molecules are used to modify CdV_2O_6, the peroxidase-like activity of PDI-CdV_2O_6 composites will be greatly enhanced. To the best of our knowledge, there are few reports on the determination of PG by colorimetric method based on PDI-CdV_2O_6 nanozyme.

Herein, CdV_2O_6 nanorods were firstly found to possess the peroxidase-like activity. Furthermore, a conjugate organic molecule, PDI was used to modify CdV_2O_6 nanorods to improve the catalytic activity and robust stability greatly. As expected, the peroxidase-like activity and robust stability of PDI-CdV_2O_6 were indeed higher than that of pure CdV_2O_6. Notably, PDI-CdV_2O_6 as the artificial nanozyme can effectively catalyze the chromogenic substrate TMB to be oxidized by H_2O_2 only in 90 s, and remains more than 70% catalytic activity over a wide range of 15 to 60 °C. The catalytic mechanism was investigated by free radical trapping and fluorescence experiments, respectively. Thus, a fast cheap colorimetric platform based on PDI-CdV_2O_6 nanorods was established for H_2O_2 and PG determination.

Experimental section

Materials

NH_4VO_3, $CdCl_2$•$2.5H_2O$, Ethylenediaminetetraacetic acid disodium salt (EDTA), isopropanol (IPA), terephthalic acid (TA), p-benzoquinone (PBQ), H_2O_2 (30 wt%), NaCl, $BaCl_2$, KCl and urea, were purchased from Sinopharm Chemical Reagent Co., Ltd. (Shanghai, China). Pyrogallol (PG) was acquired from Shanghai Ekear Biotechnology Co., Ltd. 3,3,5,5-Tetramethylbenzidine (TMB), D-Histidine (His), D-Serine (Ser), L-Arginine (Arg), lactose, leucine, fructose and sucrose were purchased from Sigma-Aldrich Co., LLC. N, N-dicarboxymethyl Perylenediimide (Fig. S1) was synthesis according the previous report [23].

Instruments

Details about instruments are presented in supporting information.

Preparation

Preparation of CdV_2O_6 The CdV_2O_6 nanorods was synthesized according to previous reports [24]. The detailed procedure is presented in supporting information.

Preparation PDI-CdV_2O_6 2 mg PDI was dissolved in 10 mL deionized water, and 100 mg CdV_2O_6 was added into 80 mL deionized water. Take 2 mL 0.4 mM PDI sample add to CdV_2O_6 solution. After 30 min of ultrasound at room temperature, the reaction system was moved into a 100 mL of autoclave and maintained for 2 h at 110 °C. Then, the precipitate was collected by centrifugation (10,000 r/min, 11,180 g) and washed with water and ethanol for several times. Finally, the product was dried overnight at 60 °C. Thus, PDI-CdV_2O_6 were successfully prepared.

Assay of the catalytic mechanism

To study the generation of active free radicals, holes (h^+), superoxide radicals ($\bullet O_2^-$), and hydroxyl radicals (•OH) are scavenged by EDTA, PBQ and IPA, respectively. Specifically, adding 200 μL scavengers into TMB-H_2O_2 reaction systems reacted for 90 s under the optimal conditions, and then recording the absorbance at 652 nm.

Fluorescent experiments were implemented by using TA (hydroxyterephthalic acid) as a fluorescence probe to further explore whether hydroxyl radicals (•OH) was produced. TA could easily react with •OH to form a high fluorescence product, dihydroxyterephthalic acid (HOTA). Specifically, phosphate buffer (pH = 4.0), the aqueous solution of PDI-CdV_2O_6 with different concentration (0.1–0.8 mg/mL), 25 mM H_2O_2 and fresh TA (5 mM) were added into quartz cuvette. After reacted for 30 min, the fluorescence spectra were reported. The fixed excitation wavelength is 315 nm, and the strongest signal appears around 440 nm.

The detailed experiments

Assays of the peroxidase-like activity, steady-state kinetics of PDI-CdV_2O_6 and colorimetric determination of H_2O_2 and PG, are provided in the supporting information.

Determination of H_2O_2 and PG in real samples

Determination of H_2O_2 in milk samples Milk was purchased from our local supermarket (Qingdao, China). First of all, 5 mL milk was diluted to 50 mL with deionized water and centrifuged at 10,000 rpm to eliminate the organic components. Next, the supernatant was filtrated through a 0.45 μm filtered membrane and then different concentrations of H_2O_2 (200 μL) were added to the supernatant. Subsequently, 200 μL of 1 mM TMB was added to the reaction system containing buffer, PDI-CdV_2O_6 and the milk sample. After incubated for 90 s at the optimal temperature (45 oC), the absorbance (652 nm) of solutions was reported on a UV–vis spectrophotometer.

Determination of PG in tap water The tap water, from our laboratory from Shandong University of Science and Technology, was treated by being centrifuged (10,000 r/min) and filtered through a 0.2 μm membrane. Subsequently, different concentrations of PG solutions were added into the treated tap water. The standard addition method was used to evaluate the practicability of the method.

Results and discussion

PDI-CdV_2O_6 characterization

Figure 1a shows the X-ray diffraction (XRD) spectra of CdV_2O_6-PDI and CdV_2O_6 nanorods, respectively. The characteristic planes (-201), (110), (-202), (201), (111), (-311), (-310), (400), (003), (311), (-403), (020), (-204), (203) are attributable to CdV_2O_6 (JCPDS card no. 22–0134). Notably, the diffraction peaks of PDI-CdV_2O_6 are similar to those of CdV_2O_6, suggesting that the introduction of PDI hardly affect the crystalline structure of CdV_2O_6.

The surface compositions of PDI-CdV_2O_6 were explored by the X-ray photoelectron spectroscopy (XPS), displayed in Fig. 1b. The total XPS spectrum reveals the presence of elements Cd, V, O and N. In the Cd 3d spectra (Fig. 1c), the peaks located at 411.3 and 404.6 eV are well corresponding to Cd $3d_{3/2}$ and Cd $3d_{5/2}$. In Fig. 1d, there are two peaks at 524.30 and 516.9 eV corresponding to the V $2p_{1/2}$ and V $2p_{2/3}$, respectively. In addition, the O 1 s spectrum (Fig. 1e) exhibits three peaks at 529.67, 530.8 and 532.28 eV, which can be assigned to the lattice oxygen, oxygen vacancy and absorbed water [25], respectively. Specially, the existence of oxygen vacancy is very important for improving the peroxidase-like activity of PDI-CdV_2O_6. Notably, in the N 1 s spectrum (Fig. 1f), the peaks at 399.8 eV can be assigned to – N – C bonds of PDI, verifying PDI molecules are successfully modified on CdV_2O_6 nanorods.

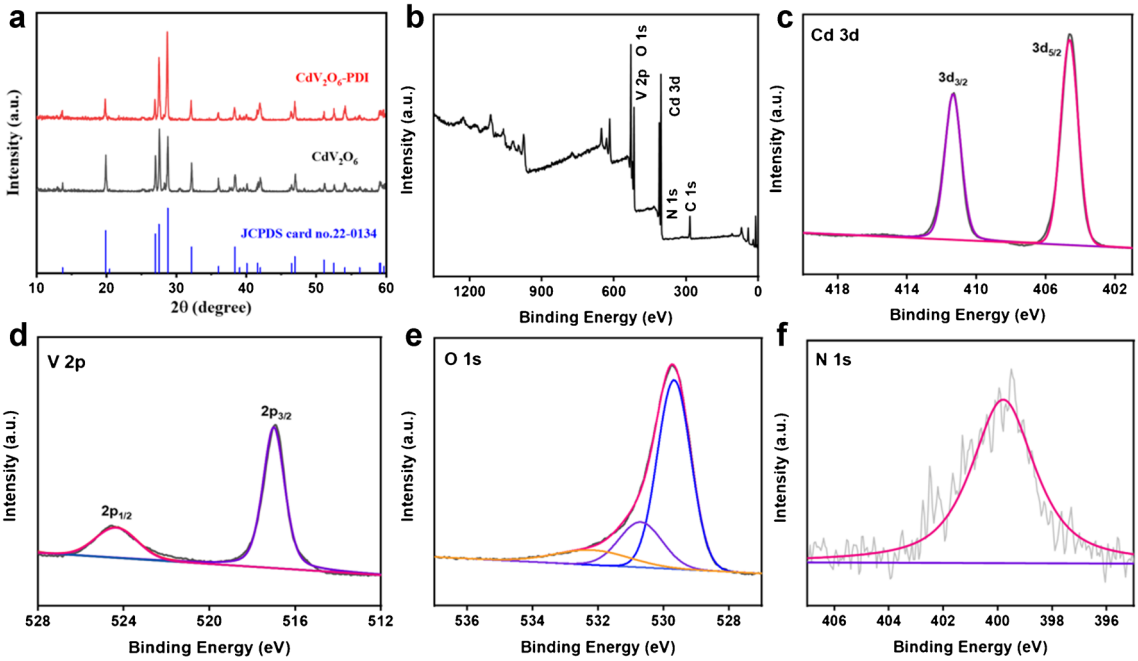

Fig. 1 XRD (a) and XPS spectra of PDI-CdV_2O_6: Survey (b), Cd 3d (c), V 2p (d), O 1 s (e) and N 1 s (f), respectively

FT-IR spectra (Fig. S2) was further confirm that the introduction of PDI molecule on CdV_2O_6 and the coordination interaction between them. Figure 2 shows SEM and TEM images of CdV_2O_6 and PDI-CdV_2O_6, respectively. From Fig. 2a and 2c, the prepared CdV_2O_6 exhibits the rod-like structure with the diameter range of 50–200 nm and an average length of 1 μm (±0.245). Also, compared with that of CdV_2O_6, the morphology of PDI-CdV_2O_6 nanorods has rarely significantly changed (Fig. 2b and 2d), because of a small amount of PDI molecules introduced.

Peroxidase-like behaviors of PDI-CdV_2O_6

The potential peroxidase-like activity of the PDI-CdV_2O_6 nanorods were investigated by using TMB-H_2O_2 reaction systems. The visible absorption spectra were recorded in the wavelength range of 500–800 nm. As presented in Fig. 3, no obvious color change of four systems (system a, b, c and d) is found, while the experimental system e (CdV_2O_6 + H_2O_2 + TMB) appears a light blue color, indicating that CdV_2O_6 possesses a weak peroxidase-like activity. Interestingly, an obvious blue change can be observed in system f, suggesting that PDI-CdV_2O_6 possesses a stronger peroxidase-like activity than that of CdV_2O_6. That is to say, the peroxidase-like activity of CdV_2O_6 is indeed greatly enhanced by the introduction of PDI molecules, ascribed to the synergistic interaction between PDI and CdV_2O_6.

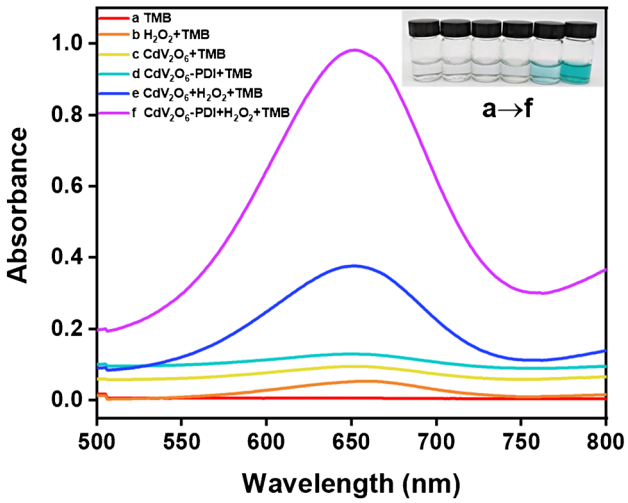

Fig. 3 UV–visible absorption spectra and corresponding photograph of color change of different reaction systems in 90 s

Optimal conditions

The catalytic activity of natural peroxidase (HRP) and reported artificial peroxidases were easily affected by pH and temperature. Thus, we studied comparatively the influences of pH and temperature on the catalytic activity of CdV_2O_6 before and after introduction of PDI (Fig. S3 and S4, number of experiment n = 3). The optimal conditions

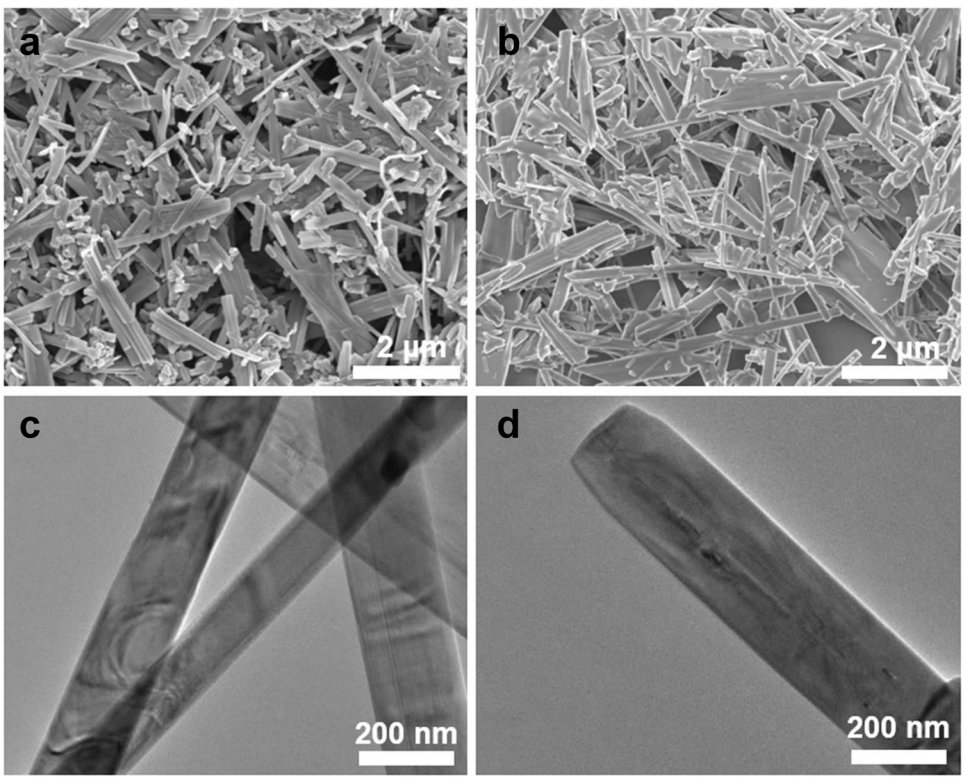

Fig. 2 SEM images of CdV_2O_6 (a) and PDI-CdV_2O_6 (b); TEM images of CdV_2O_6 (c) and PDI-CdV_2O_6 (d), respectively

are pH = 4 and 45 °C. Relevant experimental results are discussed in the supporting information.

Steady-state kinetics

To further investigate the peroxidase-like behaviors of PDI-CdV_2O_6, steady-state kinetics experiments were carried out. Fig. S5a and S5b show the typical Michaelis–Menten plots towards substrates TMB and H_2O_2, respectively. The kinetic parameters (K_m and V_{max}) were calculated and listed in Table 1, according to the double-reciprocal linear Weaver Burk plots (Fig. S5c and S5d). As we know, K_m is associated with the affinity between peroxidase mimics and substrates. As shown in Table 1, the K_m values of PDI-CdV_2O_6 nanorods with TMB and H_2O_2 are 0.129 and 2.053 mM, respectively, much lower than that of HRP [26] and other artificial enzymes. Specifically, the K_m value of PDI-CdV_2O_6 nanorods for TMB is 62 times lower than that of $AgVO_3$ [27], 10 times lower than that of NiV_2O_6 [28] and 6.5 times lower than that of $ZnFeO_4$ [29], suggesting a much stronger affinity of PDI-CdV_2O_6 towards TMB.

Catalytic mechanism

According to the previous studies, one of the catalytic mechanisms of artificial peroxidase mimics is ascribed to active species. Above all, to determine whether •OH occurred in the catalytic reaction, TA was selected as a fluorescence probe, which can easily react with •OH to produce a remarkable fluorescent hydroxy terephthalate acid. As seen from Fig. 4a, the fluorescence intensity decreases with increasing of the amount of PDI-CdV_2O_6, indicating no •OH production during the catalytic reaction.

Furthermore, active free radicals capture experiments were carried out by using PBQ, EDTA and IPA as scavengers to capture $•O_2^-$, h^+ and •OH, respectively. As seen from Fig. 4b, the catalytic activity of PDI-CdV_2O_6 is decreased apparently after adding PBQ and decreased slightly after adding EDTA, while IPA have negligible effect during the catalytic reaction. Thereof, $•O_2^-$ can be verified to be the primary active species during the catalytic reaction in the presence of PDI-CdV_2O_6.

To further explore the catalytic mechanism, the electron transport direction between CdV_2O_6 and PDI is obtained by measuring the forbidden bandwidth (E_g) and valence band (VB) of CdV_2O_6 with UV–vis diffuse reflection and XPS. E_g and VB value of CdV_2O_6 are determined to be 2.53 and 2.14 eV (Fig. 5c and 5d), as well as the conduction band (CB) is calculated to be -0.39 eV.

Based on the experimental data above, the catalytic mechanism of PDI-CdV_2O_6 was proposed (Scheme 1). As a typical photosensitizer, PDI molecules have relatively strong absorption in the visible region. Initially, the CB of CdV_2O_6 is higher than that of PDI, so electrons can be transferred from CdV_2O_6 to PDI under the irradiation of natural light, forming an electric field and facilitating the separation of electron and hole. The holes in VB of PDI with strong oxidation ability are transferred to CdV_2O_6 to further oxidize H_2O_2, generating H_2O and O_2. Thus, because a lot of oxygen vacancies existed in PDI-CdV_2O_6, the transferred electrons are captured by oxygen dissolved in the solution, and accelerates the generation of reactive oxygen ($•O_2^-$), which can easily catalyze the substrate TMB into blue oxTMB. The reducibility of pyrogallol with different concentration can fade the blue color of oxTMB to different extent. Thus, the concentration of pyrogallol can be determined, according to the intensity of absorption of oxTMB at 652 nm.

Table 1 Comparison of kinetic parameters (K_m and V_{max}) of different peroxidase mimics

Catalyst	K_m/mM		$V_{max}/10^{-8}$ Ms^{-1}		Ref
	TMB	H_2O_2	TMB	H_2O_2	
NiV_2O_6	1.359	1.747	0.904	0.412	[28]
HRP	0.434	3.70	10.0	8.71	[26]
$ZnFeO_4$	0.85	1.66	13.31	7.14	[29]
$AgVO_3$	8.03	14	-	-	[27]
PDI-CdV_2O_6	0.129	2.053	19.7	7.71	This work

Determination of H_2O_2 and PG

Based on the excellent peroxidase-like activity of PDI-CdV_2O_6, a facile colorimetric sensing platform was established to determination H_2O_2 and PG, respectively. From Fig. 5a, it can be found that the absorbance increases gradually as increasing the concentration of H_2O_2. Figure 5b shows a good linear correlation between the absorbance and H_2O_2 concentration in the range of 50–100 μM ($R^2 = 0.9993$) and the detection limit (LOD) is calculated to be 36.5 μM (LOD = 3 s/k). The comparison of LOD with other sensors based on different nanomaterials (PA/$Cu_3(PO_4)_2$•$3H_2O$ [30], TPyP-CuS [31] NiO/a-Fe_2O_3 [32], CuS [33], PDDA-AgNPs [34] and Ir NPs [35]), shown in Table S1.

Pyrogallol, one of the phenol hydroxyl groups, as a reductant molecule, can significantly inhibit the oxidation of TMB and make the blue color of ox-TMB faded. Based on this theory, a fast cheap colorimetric method was used to determination pyrogallol. Figure 5c shows a typical dose-respond plot of the absorbance at 652 nm and the concentration of PG from 1 to 80 μM. Figure 5d shows the linear range of PG deterimination in the range of 1–10 μM. The detection limit is calculated as 0.179 μM, which was 55 times, 10 times and 2 times lower than that of reported colorimetric sensors based nanozymes including Ch-Ag NPs [36], Cu,N@C-dots [37] and Au-NPs [38], respectively. Our determination limit was even lower than that of some

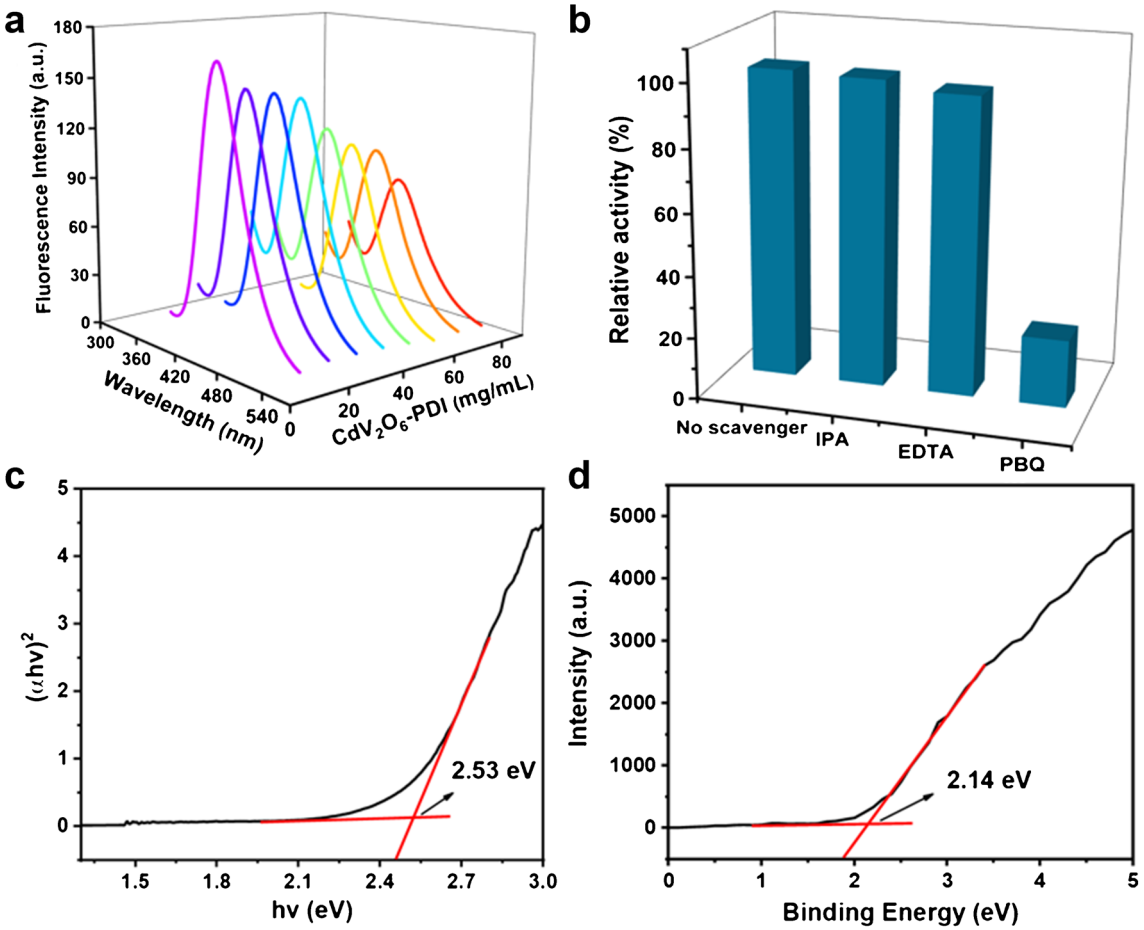

Fig. 4 (a) Fluorescence intensity varies with the concentration of PDI-CdV_2O_6 at different wavelengths. (b) Effect of scavengers on the removal capacity of reactive species. (c) Band gaps and (d) XPS-VB of CdV_2O_6

electrochemical assays (Preanodized SPCE [39], CoPc/SPCE [40]) known as the high sensitivity, as well as slightly higher than that of chemiluminescence method (N-CDs[18]), listed in Table 2. Therefore, the constructed colorimetric sensor of PG exhibited a good sensitivity.

The selectivity of this method for H_2O_2 and PG sensing

The selectivity is important to evaluate the anti-interference performance of the constructed colorimetric sensor. Thereof, different interfering substances including Na^+, K^+, Ba^{2+}, Suc, Lac, Fru, Arg, Ser, His, UA and Leu were added into the catalytic systems, respectively. From Fig. 6a and 6b, absorbance difference value ΔA ($\Delta A = A_{blank} - A_{sub}$) of two systems containing H_2O_2 and PG are much higher than that of other interferents, even though the concentrations of interfering substances are 10 times that of H_2O_2 and 100 times that of PG, respectively. As seen from Fig. S6, the good selectivity of the colorimetric method in determination of H_2O_2 and pyrogallol.

Furthermore, the stability of CdV_2O_6 and PDI-CdV_2O_6 were investigated by centrifugally recycling and testing the peroxidase-like activity (Fig. S7). The relative activity of PDI-CdV_2O_6 remains more than 75% after reusing for six times, while CdV_2O_6 remains less than 40%. It is suggested that the stability of CdV_2O_6 has been improved by introducing PDI molecules as well as the colorimetric sensing platform based on PDI-CdV_2O_6 exhibits stable performance.

Determination of H_2O_2 and PG in real samples

The practicability of the established colorimetric sensors was investigated by detecting for H_2O_2 in milk and PG in tap water (Table S2 and S3). As can be seen from these Tables, the recovery of H_2O_2 and PG is 98.90–102.94% and 103.68–105.07%, and the relative standard deviation (RSD) is calculated below 1.79% and 1.34% for H_2O_2 and PG, respectively. It is indicated that PDI-CdV_2O_6-based colorimetric sensors of H_2O_2 and PG have the potential application in determining of real samples.

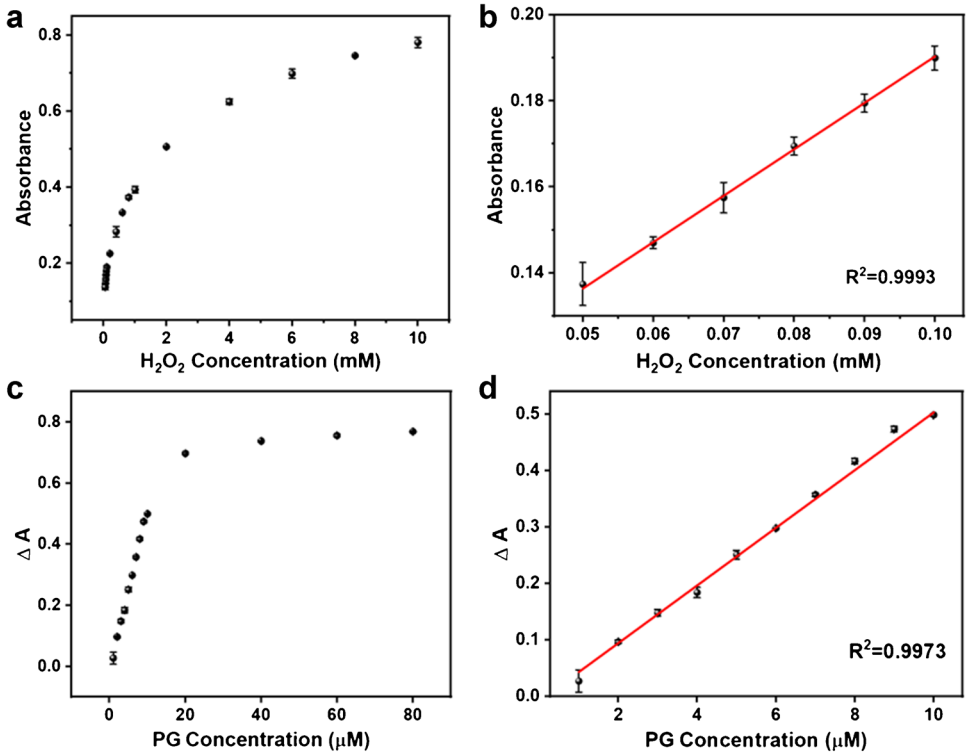

Fig. 5 (a) A dose–response plot depending of the absorbance at 652 nm on the concentration of H_2O_2 from 0.05 mM to 10 mM; (b) The corresponding linear calibration plot of H_2O_2; (c) A dose–response plot depending on the absorbance of ox-TMB at 652 nm on the concentration of PG from 1 μM to 80 μM; (d) The corresponding linear calibration plot of PG

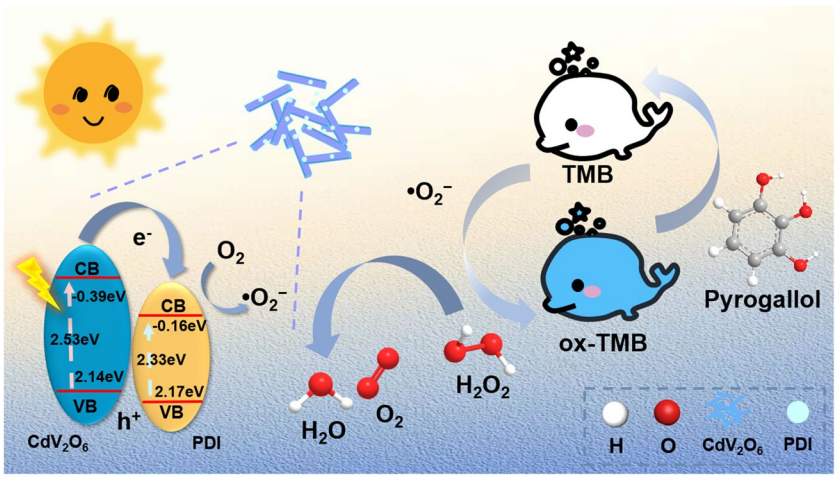

Scheme 1 The schematic diagram of PDI-CdV_2O_6 nanorods as a peroxidase mimic for PG determination

Table 2 Determination limit of PG by different methods based nanomaterials

Materials	Linear range (μM)	LOD (μM)	Method	Ref
Ch-Ag NPs	10–10,000	10	Colorimetry	[36]
Cu,N@C-dots	6–140	1.8	Colorimetry	[37]
Au-NPs	0.6–100	0.32	Colorimetry	[38]
Preanodized SPCE	10–1000	0.33	Electrochemistry	[39]
CoPc /SPCE	10–100	2.44	Electrochemistry	[40]
PDI-CdV_2O_6	1–10	0.179	Colorimetry	This work
N-CDs	0.1–100	0.046	Chemiluminescence	[18]

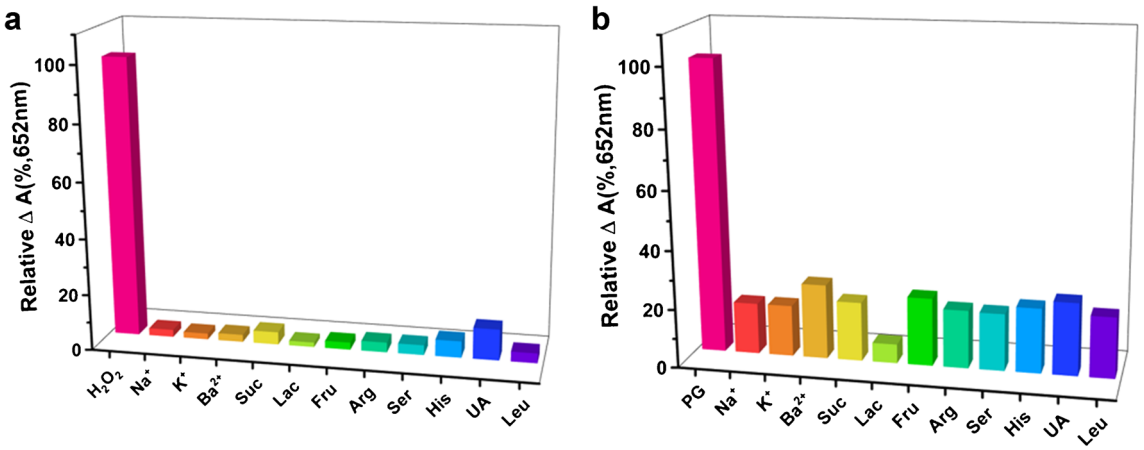

Fig. 6 The selectivity of the colorimetric sensor based on PDI-CdV_2O_6 for H_2O_2 and PG determination

Conclusions

In a word, the peroxidase-like activity and the robust stability of CdV_2O_6 have been significantly increased via modification with PDI molecules. PDI-CdV_2O_6 nanorods rapidly catalyze the oxidation of TMB in the presence of H_2O_2 only in 90 s. The peroxidase-like activity of PDI-CdV_2O_6 remains more than 70% catalytic activity over a wide range of 15 to 60 °C, ascribed to the synergetic effect between CdV_2O_6 and PDI. Based on the excellent catalytic activity of PDI-CdV_2O_6 nanozyme, a rapid colorimetric sensor for determination of H_2O_2 and PG has been constructed and has been successfully used in determination of H_2O_2 in milk and PG in tap water. This constructed colorimetric sensor has the potential application in fields of food, nanotechnology, medicine and environment.

Supplementary Information The online version contains supplementary material available at https://doi.org/10.1007/s00604-023-05846-4.

Acknowledgements This work was supported by the National Natural Science Foundation of China (Grant No. 21971152), Shandong Key Laboratory of Biochemical Analysis (SKLBA2207) and the Project of Shandong Province Higher Educational Young Innovative Talent Introduction and Cultivation Team [Nanozymes Biomedical Innovation Team].

Data Availability Data openly available in a public repository.

Declarations

Conflict of interest The authors declare that they have no conflict of interest.

References

1. Song C, Ding W, Zhao W, Liu H, Wang J, Yao Y, Yao C (2020) High peroxidase-like activity realized by facile synthesis of FeS_2 nanoparticles for sensitive colorimetric detection of H_2O_2 and glutathione. Biosens Bioelectron 151:111983. https://doi.org/10.1016/j.bios.2019.111983
2. Li N, Liu M, Ma Y, Chang Q, Wang H, Li Y, Zhang H, Liu B, Xue C, Hu S (2021) Molybdenum Selenide/Porous Carbon Nanomaterial Heterostructures with Remarkably Enhanced Light-Boosting Peroxidase-like Activities. ACS Appl Mater Interfaces 13:54274–54283. https://doi.org/10.1021/acsami.1c16569
3. Li R, Zhou Y, Zou L, Li S, Wang J, Shu C, Wang C, Ge J, Ling L (2017) In situ growth of gold nanoparticles on hydrogen-bond supramolecular structures with high peroxidase-like activity at neutral pH and their application to one-pot blood glucose sensing. Sens Actuators, B Chem 245:656–664. https://doi.org/10.1016/j.snb.2017.01.141
4. Chen M, Sun L, Ding Y, Shi Z, Liu Q (2017) N, N′-Dicarboxymethyl perylene diimide functionalized magnetic nanocomposites with enhanced peroxidase-like activity for colorimetric sensing of $_H2_O2$ and glucose. New J Chem 41:5853–5862. https://doi.org/10.1039/c7nj00292k
5. Feng L, Zhang L, Chu S, Zhang S, Chen X, Du Z, Gong Y, Wang H (2022) Controllable doping of Fe atoms into MoS2 nanosheets towards peroxidase-like nanozyme with enhanced catalysis for colorimetric analysis of glucose. Appl Surf Sci 583:152496. https://doi.org/10.1016/j.apsusc.2022.152496
6. Liang Y, Li H, Fan L, Li R, Cui Y, Ji X, Xiao H, Hu J, Wang L (2022) Zwitterionic daptomycin stabilized palladiumnanoparticles with enhanced peroxidase-like properties for glucose detection. Colloids and Surfaces A: Physicochemical and Engineering Aspects 633:127797. https://doi.org/10.1016/j.colsurfa.2021.127797
7. Wang Y, Liu X, Wang M, Wang X, Ma W, Li J (2021) Facile synthesis of CDs@ZIF-8 nanocomposites as excellentperoxidase mimics for

colorimetric detection of H2O2 and glutathione. Sens Actuators B: Chemi 329:129115. https://doi.org/10.1016/j.snb.2020.129115
8. Li J, Zhao J, Li S, Chen Y, Lv W, Zhang J, Zhang L, Zhang Z, Lu X (2021) Synergistic effect enhances the peroxidase-like activity in platinum nanoparticle-supported metal-organic framework hybrid nanozymes for ultrasensitive detection of glucose. Nano Res 14:4689–4695. https://doi.org/10.1007/s12274-021-3406-z
9. Nguyen PT, Lee J, Cho A, Kim MS, Choi D, Han JW, Kim MI, Lee J (2022) Rational development of co-doped mesoporous ceria with high peroxidase-mimicking activity at neutral ph for paper-based colorimetric detection of multiple biomarkers. Adv Funct Mater 32:2112428. https://doi.org/10.1002/adfm.202112428
10. Tran HV, Nguyen ND, Tran CTQ, Tran LT, Le TD, Tran HTT, Piro B, Huynh CD, Nguyen TN, Nguyen NTT, Dang HTM, Nguyen HL, Tran LD, Phan NT (2020) Silver nanoparticles-decorated reduced graphene oxide: A novel peroxidase-like activity nanomaterial for development of a colorimetric glucose biosensor. Arab J Chem 13:6084–6091. https://doi.org/10.1016/j.arabjc.2020.05.008
11. Wei F, Cui X, Wang Z, Dong C, Li J, Han X (2021) Recoverable peroxidase-like Fe_3O_4@MoS_2-Ag nanozyme with enhanced antibacterial ability. Chem Eng J 408:127240. https://doi.org/10.1016/j.cej.2020.127240
12. Zhu X, Li H, Zhang D, Chen W, Fu M, Nie S, Gao Y, Liu Q (2019) Novel "On–Off" Colorimetric Sensor for Glutathione Based on Peroxidase Activity of Montmorillonite-Loaded TiO_2 Functionalized by Porphyrin Precisely Controlled by Visible Light. ACS Sustainable Chemistry & Engineering 7:18105–18113. https://doi.org/10.1021/acssuschemeng.9b05146
13. Zhang L, Chen M, Jiang Y, Chen M, Ding Y, Liu Q (2017) A facile preparation of montmorillonite-supported copper sulfide nanocomposites and their application in the detection of H_2O_2. Sens Actuators, B Chem 239:28–35. https://doi.org/10.1016/j.snb.2016.07.168
14. Liu Q, Yang Y, Li H, Zhu R, Shao Q, Yang S, Xu J (2015) NiO nanoparticles modified with 5,10,15,20-tetrakis(4-carboxyl pheyl)-porphyrin: promising peroxidase mimetics for H_2O_2 and glucose detection. Biosens Bioelectron 64:147–153. https://doi.org/10.1016/j.bios.2014.08.062
15. Lyu H, Yin D, Zhu B, Lu G, Liu Q-Y, Zhang X, Zhang X (2020) Metal-Free 2(3),9(10),16(17),23(24)-Octamethoxyphthalocyanine-Modified Uniform CoSn(OH)6 Nanocubes: Enhanced Peroxidase-like Activity, Catalytic Mechanism, and Fast Colorimetric Sensing for Cholesterol. ACS Sustainable Chemistry & Engineering 8:9404–9414. https://doi.org/10.1021/acssuschemeng.0c02151
16. Ding K, Wang Y, Shan T, Xu J, Bao Q, Liu F, Zhong H (2020) Propeller-like acceptors with difluoride perylene diimides for organic solar cells. Organic Electronics 78:105569. https://doi.org/10.1016/j.orgel.2019.105569
17. Wurthner F, Saha-Moller CR, Fimmel B, Ogi S, Leowanawat P, Schmidt D (2016) Perylene Bisimide Dye Assemblies as Archetype Functional Supramolecular Materials. Chem Rev 116:962–1052. https://doi.org/10.1021/acs.chemrev.5b00188
18. Shah SN, Li H, Linv JM (2016) vEnhancement of periodate-hydrogen peroxide chemiluminescence by nitrogen doped carbon dots and its application for the determination of pyrogallol and gallic acid. Talanta 153:23–30. https://doi.org/10.1016/j.talanta.2016.02.056
19. Li Z, Yang Y, Zeng Y, Wang J, Liu H, Guo L, Li L (2017) Novel imidazole fluorescent poly(ionic liquid) nanoparticles for selective and sensitive determination of pyrogallol. Talanta 174:198–205. https://doi.org/10.1016/j.talanta.2017.06.007
20. Vafaei A, Bin Mohamad J, Karimi E (2019) HPLC profiling of phenolics and flavonoids of Adonidia merrillii fruits and their antioxidant and cytotoxic properties. Nat Prod Res 33:2531–2535. https://doi.org/10.1080/14786419.2018.1448810
21. Raghu P, Madhusudana Reddy T, Reddaiah K, Jaidev LR, Narasimha G (2013) A novel electrochemical biosensor based on horseradish peroxidase immobilized on Ag-nanoparticles/poly(l-arginine) modified carbon paste electrode toward the determination of pyrogallol/hydroquinone. Enzyme Microb Technol 52:377–385. https://doi.org/10.1016/j.enzmictec.2013.02.010
22 Mostafa IM, Gilani M, Chen Y, Lou B, Li J, Xu G (2021) Lucigenin-pyrogallol chemiluminescence for the multiple detection of pyrogallol, cobalt ion, and tyrosinase. J Food Drug Anal 29:510–520. https://doi.org/10.38212/2224-6614.3361
23. Gebers J, Rolland D, Marty R, Suarez S, Cervini L, Scopelliti R, Brauer JC, Frauenrathv H (2015) Solubility and crystallizability: facile access to functionalized pi-conjugated compounds with chlorendylimide protecting groups. Chemistry 21:1542–1553. https://doi.org/10.1002/chem.201403623
24. Li D, Bai X, Pan C, Zhu Y (2013) Investigations on the Phase Transition between CdV_2O_6 and $Cd_2V_2O_7$ and Their Photocatalytic Performances. Eur J Inorg Chem 2013:3070–3075. https://doi.org/10.1002/ejic.201300020
25. Jia R, Wang Y, Wang C, Ling Y, Yu Y, Zhang B (2020) Boosting Selective Nitrate Electroreduction to Ammonium by Constructing Oxygen Vacancies in TiO_2. ACS Catal 10:3533–3540. https://doi.org/10.1021/acscatal.9b05260
26. Gao L, Zhuang J, Nie L, Zhang J, Zhang Y, Gu N, Wang T, Feng J, Yang D, Perrett S, Yan X (2007) Intrinsic peroxidase-like activity of ferromagnetic nanoparticles. Nat Nanotechnol 2:577–583. https://doi.org/10.1038/nnano.2007.260
27. Xiang Z, Wang Y, Ju P, Zhang D (2015) Optical determination of hydrogen peroxide by exploiting the peroxidase-like activity of $AgVO_3$ nanobelts. Microchim Acta 183:457–463. https://doi.org/10.1007/s00604-015-1670-x
28. Zhu Q, Yang J, Peng Z, He Z, Chen W, Tang H, Li Y (2021) Selective detection of glutathione by flower-like NiV_2O_6 with only peroxidase-like activity at neutral pH. Talanta. 234:122645. https://doi.org/10.1016/j.talanta.2021.122645
29. Su L, Feng J, Zhou X, Ren C, Li H, Chen X (2012) Colorimetric detection of urine glucose based $ZnFe_2O_4$ magnetic nanoparticles. Anal Chem 84:5753–5758. https://doi.org/10.1021/ac300939z
30. Zhang CY, Zhang H, Yang FQ (2021) Enhanced peroxidase-like activity of copper phosphate modified by hydrophilic phytic-acid and its application in colorimetric detection of hydrogen peroxide. Microchem J168:106489. https://doi.org/10.1016/j.microc.2021.106489
31. He Y, Li N, Lian L, Yang Z, Liu Z, Liu Q, Zhang X, Zhang X (2020) Colorimetric ascorbic acid sensing from a synergetic catalytic strategy based on 5,10,15,20-tetra(4-pyridyl)-21H,23H-porphyrin functionalized CuS nanohexahedrons with the enhanced peroxidase-like activity. Colloids and Surfaces A: Physicochemical and Engineering Aspects 598:124855. https://doi.org/10.1016/j.colsurfa.2020.124855
32. Achari DS, Santhosh C, Deivasegamani R, Nivetha R, Bhatnagar A, Jeong SK, Grace AN (2017) A non-enzymatic sensor for hydrogen peroxide based on the use of α-Fe_2O_3 nanoparticles deposited on the surface of NiO nanosheets. Microchimica Acta 184:3223–3229. https://doi.org/10.1007/s00604-017-2335-8
33. Guan J, Peng J, Jin X (2015) Synthesis of copper sulfide nanorods as peroxidase mimics for the colorimetric detection of hydrogen peroxide. Anal Methods 7:5454–5461. https://doi.org/10.1039/c5ay00895f
34. Rivero PJ, Ibañez E, Goicoechea J, Urrutia A, Matias IR, Arregui FJ (2017) A self-referenced optical colorimetric sensor based on silver and gold nanoparticles for quantitative determination of hydrogen peroxide. Sens Actuators, B Chem 251:624–631. https://doi.org/10.1016/j.snb.2017.05.110
35. Cui M, Zhou J, Zhao Y, Song Q (2017) Facile synthesis of iridium nanoparticles with superior peroxidase-like activity for

colorimetric determination of H_2O_2 and xanthine. Sens Actuators, B Chem 243:203–210. https://doi.org/10.1016/j.snb.2016.11.145
36. Chen Z, Zhang X, Cao H, Huang Y (2013) Chitosan-capped silver nanoparticles as a highly selective colorimetric probe for visual detection of aromatic ortho-trihydroxy phenols. Analyst 138:2343–2349. https://doi.org/10.1039/c3an36905f
37. Ali HRH, Hassan AI, Hassan YF, El-Wekil MM (2019) Colorimetric and fluorimetric (dual-mode) nanoprobe for the determination of pyrogallol based on the complexation with copper(II)- and nitrogen-doped carbon dots. Mikrochim Acta 186:850. https://doi.org/10.1007/s00604-019-3892-9
38. Nezhad MR, Alimohammadi M, Tashkhourian J, Razavian SM (2008) Optical detection of phenolic compounds based on the surface plasmon resonance band of Au nanoparticles. Spectrochim Acta A Mol Biomol Spectrosc 71:199–203. https://doi.org/10.1016/j.saa.2007.12.003
39. Feng P-S, Wang S-M, Su W-Y, Cheng S-H (2012) Electrochemical Oxidation and Sensitive Determination of Pyrogallol at Preanodized Screen-Printed Carbon Electrodes. J Chin Chem Soc 59:231–238. https://doi.org/10.1002/jccs.201100384
40. Matemadombo F, Apetrei C, Nyokong T, Rodríguez-Méndez ML, de Saja JA (2012) Comparison of carbon screen-printed and disk electrodes in the detection of antioxidants using CoPc derivatives. Sens Actuators, B Chem 166–167:457–466. https://doi.org/10.1016/j.snb.2012.02.088